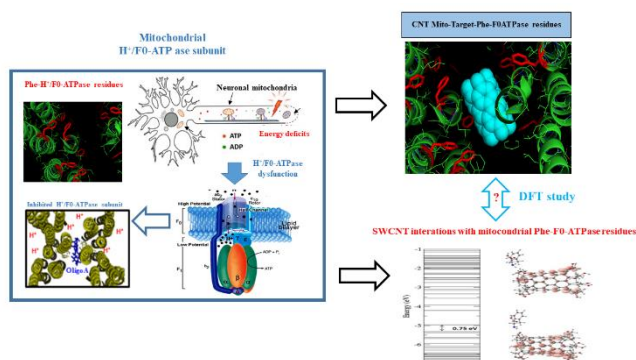# Precision Medicine: Carbon Nanotubes as Potential Treatment for Human Brain Disorders-Based Mitochondrial Dysfunctions with a First Principles DFT-Study

<Patrícia Viera de Oliveira> (E-mail:patiolivera@yahoo.com.br) [a],

< Michael Gonzalez Durruthy > (E-mail: gonzalezdurruthy.furg@gmail.com)[b],

< José María Monserrat> (E-mail: josemmonserrat@gmail.com)[c] ,

< Solange Binotto Fagan> (E-mail: solange.fagan@gmail.com)[d]

[a, d] <[1]Centro Universitário Franciscano (UNIFRA), Postgraduate Program in Nanoscience, Santa Maria, RS, Brazil >

[b,c] <[2]Institute of Biological Sciences (ICB)-Federal University of Rio Grande - FURG, Postgraduate Program in Physiological Sciences, Rio Grande, RS, Brazil>

Graphical Abstract

Abstract.

The study of key molecular mechanisms of mitochondrial dysfunctions, which are responsible for neurodegenerative diseases, is a critical step to assist for the diagnosis and therapy success. In this regard, we suggest an alternative of treatment on neurodegenerative disorders-based on Single-Walled Carbon Nanotubes (SWCNT) as potential mito protective -(Phe)-F0-ATPase targeting nanoparticles toward Precision Molecular Nanomedicine against pathological ATP-hydrolysis conditions. Herein, we used *ab initio* computational simulation to analyze the structural and electronic properties from SWCNT-family with zigzag topologies (n, m - Hamada indices n > 0; m = 0) like: SWCNT-pristine, SWCNT-COOH, SWCNT-OH, SWCNT-monovacancy interacting with the critical (Phe)-residues of the mitochondrial F0-ATPase and using oligomycin A (specific Phe-F0-ATPase inhibitor) as reference control. Then, we show that the SWCNT-family can be potentially used to selectively inhibit the (Phe)-F0-ATPase activity liked to pathological mitochondrial ATP-hydrolysis associated to human neurodegenerative disorders by using DFT-*ab initio* simulation. The *in-silico* results suggest the formation of more stable complexes of interaction following the order: SWCNT-COOH/F0-ATPase complex (1.79 eV) > SWCNT-OH/F0-ATPase complex (0.61 eV) > SWCNT/F0-ATPase complex (0.45 eV) > SWCNT-monovacancy/F0-ATPase complex (0.43 eV) based on the strength of the

	chemisorption interactions. These theoretical evidences open new horizons towards mito-target precision nanomedicine.

Introduction

Neurodegenerative diseases are morphologically characterized, by the selective and progressive loss of neuronal tissue. These neurodegenerative disorders like: Alzheimer's, Parkinson's, sclerosis and Huntington's disease have common mitochondrial mechanisms-dysfunction [1].

Mitochondrial F1F0-ATP synthase c-ring subunit produces ATP from (ADP + Pi) in the presence of an H^+-proton gradient across the membrane which is generated by electron transport complexes of the respiratory chain. F-type ATPase's consist of two structural domains (F0 and F1). F0-containing the membrane H^+-proton channel and F1-containing the extramembraneous catalytic core toward mitochondrial intermembrane space. The F0-ATP synthase c-ring subunit structure is formed by the tens chain like A, B, C, D, E, K, L, M, N, and O. Here, oligomycin A (a specific inhibitor of F0-ATPase) can interacts with the outer and inner surface of the F0-ATP synthase c-ring subunit at a position that explains the inhibitory effect on the ATP synthesis.

Key Phenylalanine residues (Phe) from the mitochondrial F0-ATP-ase binding-site are considered as critical in mitochondrial dysfunction-based pathological ATP-hydrolysis (ADP + Pi) in (ATP) [2,3]. These residues can directly regulate the H^+-proton translocation based on great representatively in the structure aforementioned F0-ATPase chains, enabling multiple hydrophobic interactions associated to carboxyl side chains responsible for H^+-proton translocation through the F0-ATP-ase subunit.

Besides, the synthesis of Adenosine Triphosphate (ATP) in mitochondria is performed by a large molecular machine in the F1F0-ATP synthase. Under pathological conditions, like mitochondrial dysfunction, the Phe-residues from F0 subunit are involved in the inverse rotation that promote abrupt reduction of ATP synthesis by mitochondrial F1-ATP synthase given place the inverse process (ATP-hydrolysis syndrome). This biochemical mechanism can be inhibited by the oligomycin A Phe-F0-ATPase specific inhibitor that avoids rotation-inversion of the F0-ATPase subunit and thus cell death (apoptosis) [4,5]. The amino acid residues that form the oligomycin-binding site are 100% conserved independently of the phylogenetic position in all eukaryotic organisms.

By the other hand, the Mitochondrial Nanomedicine has been gaining prominence, especially with the use of carbon nanotubes, which are considered as promising candidates for the treatment of diseases as neuronal regeneration due to its exceptional properties on the reduction of neurotoxicity, improvement of permeability, among others [6-8]. Besides, carbon nanotubes have properties as high specific superficial area and can cross the mitochondrial outer-membrane by endocytosis and other drugs-delivery mechanisms [9].

This work aims to evaluate the structural and electronic properties of the zigzag single-walled carbon nanotube (SWCNT), SWCNT-pristine, SWCNT-COOH, SWCNT-OH and SWCNT-monovacancy interacting with critical mitochondrial binding-site (Phe)-F0ATPase residues via *ab initio* simulation. The results can help to understand the therapeutic potential of these carbon nanomaterials to prevent/inhibit the pathological ATP hydrolysis from mitochondria in the nervous system and develop new therapeutic strategies to assist in the treatment of neurodegenerative diseases.

Materials and Methods

The zigzag topologies (n > 0; m = 0) from SWCNT-OH, SWCNT-COOH, SWCNT-pristine and SWCNT-monovacancy systems were selected based on previous molecular docking studies from highly conserved pdb-X-ray crystallographic structure of the yeast F1F0 ATPase C10 ring with oligomycin A (PDB ID: 5BPS). The arrangements showed a higher reactivity / nanotoxicity-based non-covalent interaction when compared with their similar SWCNT-armchair (n = m) and SWCNT-chiral topologies (n ≠ m), and presented as the closest phenylalanine F0-ATPase residues [10]. It is important to clarify

that, c-ring-F0-ATPase subunit.pdb x-ray structure from yeats (5BPS) can be used in the context of the present theoretical approaches taking into consideration that mitochondrial c-ring-F0-ATPase subunit.pdb x-ray structure from human with oligomycin A has not been crystallized and included in the RCSB Protein Data Bank. However, the oligomycin A-pharmacodynamics mechanism is highly conserved due to the amino acid residues that form the oligomycin A-active binding site are 100% conserved between human and yeast.

This theoretical algorithm was performed to the F0-ATPase subunit using a grid box size with dimensions of X= 22 Å, Y= 22 Å, Z= 22 Å and the F0-ATPase subunit grid box center X=19.917 Å, Y= 19.654 Å, Z= 29.844 Å to evaluate the SWCNT-Phe-F0-ATPase interaction, considering the oligomycin A environment to evaluate the SWCT-affinity in the Phe-F0-ATPase subunit active binding site. The best docking final position was represented with the Pymol software.

In order to analyze the electronic and structural properties of the interacting systems (SWCNT-family member and Phe-F0-ATPase), we used the *ab initio* computational simulation methodology, which makes use of the DFT (Functional Density Theory) proposed and tested for calculations of the electronic structure of atoms, molecules and solids to chemical and physical properties [11]. To find the physical and chemical properties in the DFT, it is necessary to make use of some approximations to allow the simulation of many bodies, such as the Born-Oppenheimer approximation, pseudopotential, supercell and base function [12].

We used the SIESTA code, Spanish Initiative for Electronic Simulations with Thousands of Atoms [13] that performs self-consistent calculations to solve the Kohn-Sham equations and to evaluate the main properties resulting from the interaction between molecules and the carbon nanotubes. We used a double-base plus a polarized function (DZP), the term of exchange and correlation adopted is the Local Density Approximation (LDA) parameterized by Perdew and Zunger (1981) [14]. For the representation of the electronic space a radius of 200 Ry was used for the grid in the real space interaction, the atomic structures were relaxed until the residual forces were less than 0.05 eV/Å for all the atoms of the system. For the pseudopotential, we used the model proposed by Troullier and Martins (1991) [15].

To calculate the binding energy of the carbon nanotubes with phenylalanine or oligomycin A, equation (1) was used;

$$E = - \{[A + B] + E[A] + E[B]\} \tag{1}$$

Where [A + B] is the total energy of the system [A] (SWCNT-zigzag) that interacts with [B] (phenylalanine); and E [A], E [B] are respectively the total energy of the specific SWCNT-family member (as SWCNT-pristine, SWCNT-COOH, SWCNT-OH, SWCNT-monovacancy) and phenylalanine, isolated. For the calculation of the interaction between oligomycin A and phenylalanine, where E [A + B] total energy of the interaction oligomycin A and phenylalanine, E [A] total energetic of oligomycin A isolated and E [B] total energy of the isolated phenylalanine residue.

Results and Discussion

Next, the results obtained by computational simulation and based on molecular docking simulation are presented, as shown in Figure 1, in which the main residues involved in the interaction of BPS 5 protein with oligomycin A are highlighted.
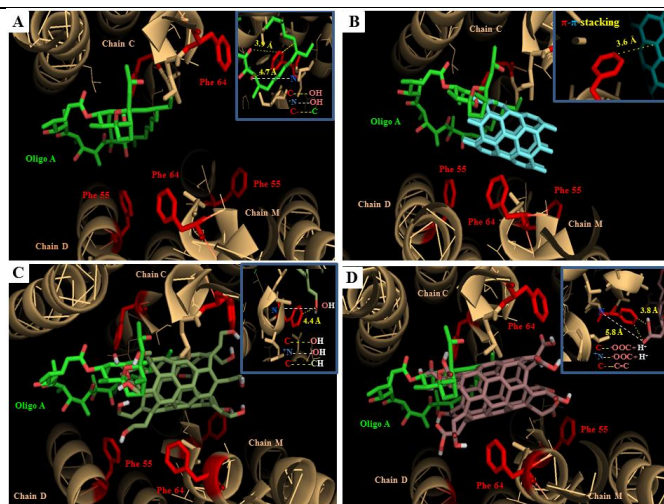
Figure 1: Cartoon representations of the best molecular docking positions obtained from modeled pristine-SWCNT and oxidized-SWCNT (SWCNT-OH and SWCNT-COOH) with critical F0-ATPase subunit-phenylalanine hydrophobic residues from the chains C, D and M showing the calculated lower interatomic distances (cutoff value ≤ 7Å; top right). A) oligomycin A as control reference (green) interacting with c-ring-F0-ATPase subunit-phenylalanine hydrophobic residues (Phe 55 and Phe 64: red). B) Pristine-SWCNT showing π-π stacking interaction with c-ring-F0-ATPase subunit-phenylalanine hydrophobic residues (Phe 55 and Phe 64: red). C) and D) SWCNT-OH and SWCNT-COOH interacting with c-ring-F0-ATPase subunit-phenylalanine hydrophobic residues (Phe 55 and Phe 64: red).
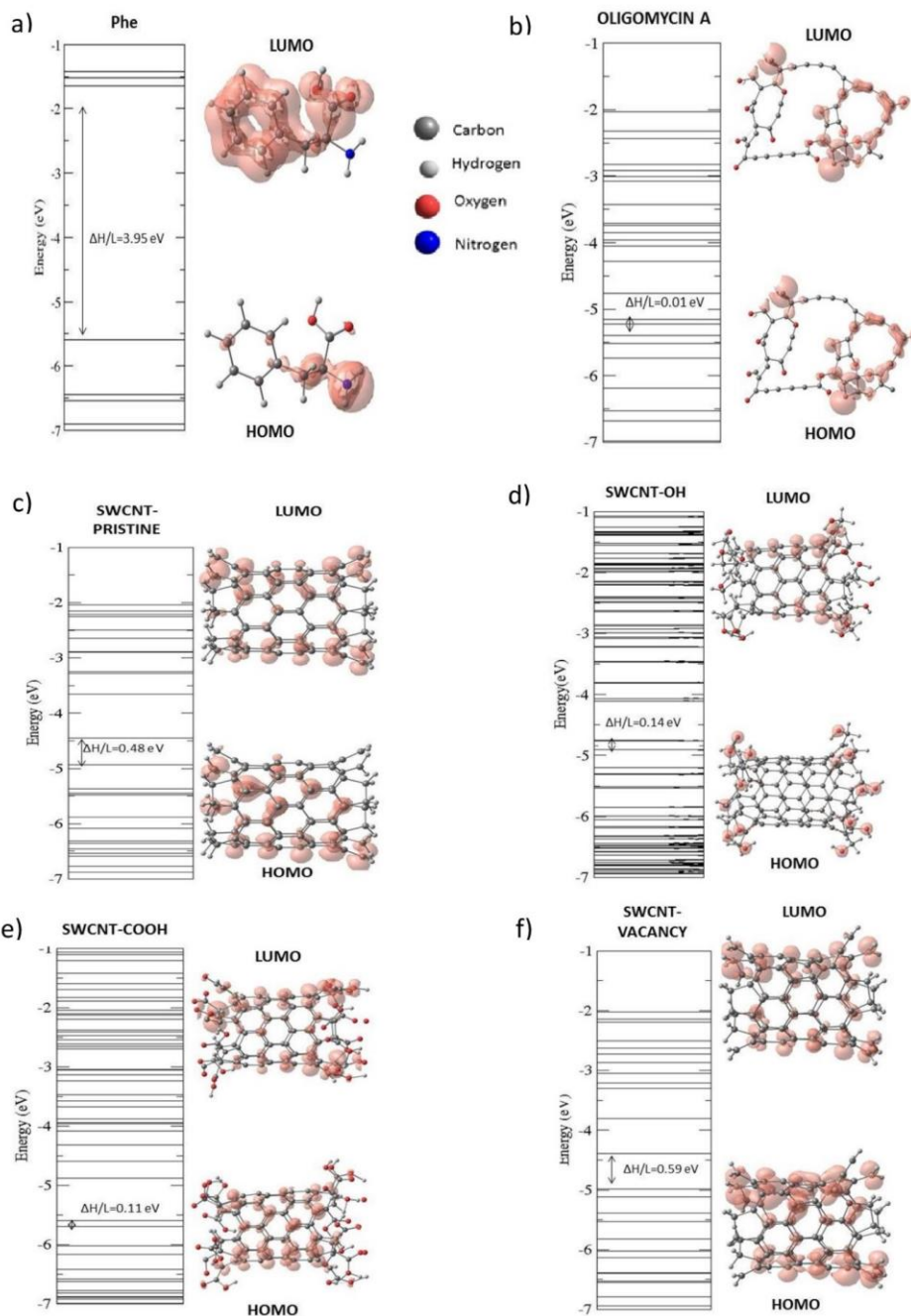
Table 1 shows lower distances between the carbon nanotubes zigzag (SWCNT-pristine, SWCNT-OH, SWCNT-COOH, SWCNT-monovacancy) and Phe-F0-ATPase and oligomycin A together with Phe-F0- ATPase (Phe-phenylalanine), numbers I, II and III represent to three different chemical arrangements for the interacting system. It is also present the values of the binding energies (according to equation 1), charge transfer, in which the positive signal of a carbon charge transfers of a Phe-F0-ATPase (Phe), the difference of HOMO (higher occupied molecular orbital) and LUMO (lowest unoccupied molecular orbital) for the isolated and interacting systems for all studied configurations.

CONFIGURATION	d (Å)	E (eV)	Δ Q (e-)	ΔH/L (eV)
Phe	-	-	-	3.95
Oligomycin A				0.01
SWCNT –OH	-	-	-	0.14
SWCNT -Pristine	-	-	-	0.48
SWCNT –COOH	-	-	-	0.11
SWCNT-Monovacancy	-	-	-	0.59
SWCNT Pristine-Phe I	2.23 H-H	0.37	-0.04	0.49
SWCNT Pristine-Phe II*	1.86 H-H	0.45	-0.08	0.43
SWCNT Pristine-Phe III	2.60 H-H	0.10	0	0.45
SWCNT -OH-Phe I*	1.86 O-H	0.61	0.06	0.75
SWCNT -OH-Phe II	1.84 O-H	0.52	0.07	0.76
SWCNT -OH-Phe III	2.45 O-H	0.51	0.06	0.76
SWCNT-COOH-Phe I	1.98 O-H	0.59	0.01	0.23
SWCNT -COOH-Phe II	2.86 O-H	0.94	0.03	0.12
SWCNT -COOH-Phe III*	1.52 N-H	1.79	-0.23	0.11
SWCNT -Monovacancy-Phe I	2.85-H-H	0.38	0.04	0.58
SWCNT -Monovacancy-Phe II*	2.62 C-H	0.43	0.11	0.58
SWCNT -Monovacancy-Phe III	2.12 H-H	0.37	0.02	0.58
Phe-Oligomycin A I*	2.17 O-H	6.44	0.16	0.26
Phe-Oligomycin A II	1.53 C-C	5.58	0.25	0.37
Phe-Oligomycin A III	1.50 O-H	4.44	0.43	0.12

Table 1: Lower binding distances for final configurations d (Å), binding energy (E(eV)), ΔQ charge transfer, and HOMO and LUMO (ΔH/L) difference. The most stable configurations of each interacting systems are highlighted with *.

By analyzing the electronic properties, we observed the energy levels of the HOMO and LUMO for phenylalanine (Figure 2 (a)). The difference between the HOMO and LUMO is 3.93 eV. The electronic charges plot show that the HOMO is concentrated in the nitrogen and carbon atoms and the LUMO in the oxygen, carbon, and hydrogen atoms of the molecule.

In the case of the oligomycin A (Figure 2 (b)), the difference between the HOMO and LUMO is 0.01 eV and the plot of electronic charge density for both the HOMO and LUMO are located at the oxygen, carbon, and hydrogen atoms. For the SWCNT-pristine, the difference between the HOMO and LUMO is 0.48 eV and the electronic charge density for both orbitals are concentrated in carbon and hydrogen atoms, (Figure 2 (c)). It is important to point out that all the SWCNT are passivated with H on the edges. By analyzing the carbon nanotube functionalized with hydroxyls (SWCNT-OH) the difference between the HOMO and LUMO is 0.17 eV and the electronic charge density for the HOMO is concentrated in the hydroxyls groups present in the edges of the nanotube and for the LUMO are concentrated on the carbon atoms from SWCNT-OH (Figure 2 (d)). Besides, the for-carbon nanotube functionalized with carboxyl (SWCNT-COOH), the difference between HOMO - LUMO is 0.11 eV and the electron density of charges for the LUMO is concentrated in the carboxylates and at the edges of the nanotube for the HOMO are concentrated on the carbon atoms of the nanotube (Figure 2 (e)). For the nanotube with vacancy (removal of a carbon atom from the nanotube), the difference HOMO-LUMO is 0.55 eV, and the electronic charge density for HOMO and LUMO are located at the place where it was removed the carbon atom and the carbon and hydrogen atoms (Figure 2 (f)).

Figures 2(a-f): Energy levels for the isolated systems, HOMO and LUMO for the following structures (a) phenylalanine, (b) oligomycin A, (c) SWCNT Pristine, (d) SWCNT -OH, (e) SWCNT -COOH and (f) SWCNT -monovacancy. The contour plot is 0.001813 eV /Å^3.

For the SWCNT-pristine interacting with the Phe-F0-ATPase, we obtained as the most stable configuration II (Figure 3 (a)), the binding energy was 0.45 eV. The intermolecular distance was 1.86 Å between the hydrogen atoms of the SWCNT-pristine and hydrogen of the phenylalanine residue from F0-ATPase, the charge transfer is 0.08 electrons that occurs from the Phe-F0-ATPase molecule to the SWCNT. The difference between the HOMO and LUMO was 0.51 eV and the electronic density of charges for HOMO and LUMO are only concentrated in the carbon nanotube, showing a weak interaction between the pristine carbon nanotube and phenylalanine.

For the interaction of oxidized-SWCNT (SWCNT-OH) interacting with Phe-F0-ATPase the most stable configuration obtained is configuration I (Figure 3 (b)) with binding energy of 0.61 eV and the shortest distance between atoms was 1.86 Å between the oxygen atoms of the carbon nanotube and hydrogen of Phe-F0-ATPase. The charge transfer is 0.06 electrons from the SWCNT to the Phe. The difference between the HOMO and LUMO is 0.28 eV, the plot for the electronic charge density for the

HOMO and LUMO are concentrated in the carbon nanotube with some hydroxyl groups, also showing a weak interaction.
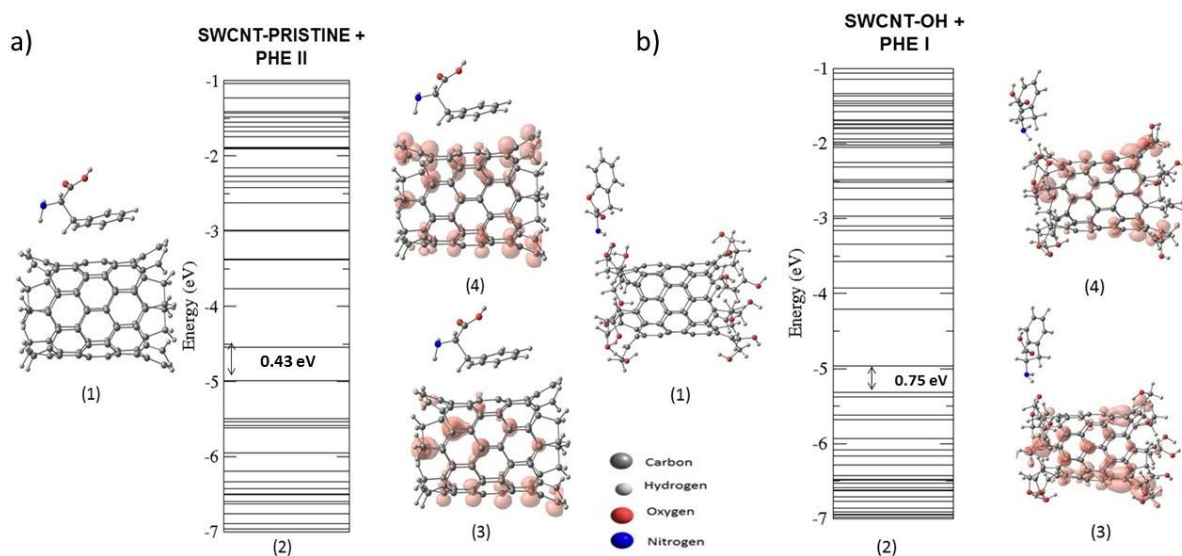

Figure 3(a-c): Most stable configurations (1), electronic levels (2), and the plot of the electronic charge density for HOMO (3) and LUMO (4) of the pristine SWCNT (a) and SWCNT-OH (b) interacting with phenylalanine. The contour plot is 0.001813 eV /Å^3.

The most stable configuration for the SWCNT-COOH interacting with Phe-F0-ATPase was shown in the Figure 4 (a), with binding energy of 0.94 eV and the distance between atoms was 2.86 Å between the oxygen atoms of the nanotube and hydrogen of Phe-F0-ATPase. The charge transfer is 0.23 electrons from the Phe-F0-ATPase molecule (F0-ATPase residue) to the SWCNT-COOH. The difference between the HOMO - LUMO is 0.12 eV with the charge concentration for the HOMO and LUMO on the carbon atoms of the nanotube, the hydroxyls, and on the phenylalanine residue.

The interaction of the SWCNT-COOH interacting with the phenylalanine and mitochondrial F0-ATPase presents higher values for the binding energy, around 1.8 eV, suggesting a chemical adsorption. This can be understood due to the modification on the HOMO and LUMO distance compared with the pristine SWCNT and also with the binding energy values. The other configurations SWCNT-pristine, SWCNT-OH and SWCNT-monovacancy with mitochondrial phenylalanine-F0-ATPase showed a binding energy of 0.45, 0.61, 0.43 eV, respectively, suggesting physical adsorption. These results corroborate the concentration of the electronic charge in HOMO and LUMO, which, for all these interactions, occurred in the SWCNT atoms and not in the phenylalanine molecule, showing a weak interaction.

The SWCNT-monovacancy interacting with Phe-F0-ATPase had the most stable configuration as shown in Figure 4 (b), with binding energy of 0.43 eV and the intramolecular distance of 2.62 Å between the carbon atoms of the nanotube and hydrogen of the Phe-F0-ATPase, the charge transfer is 0.11 electrons occurring from the SWCNT to the Phe-F0-ATPase. The difference between the HOMO and LUMO is 0.58 eV and the electronic charge density for the HOMO and the LUMO are located on the carbon and hydrogen atoms of the nanotube.
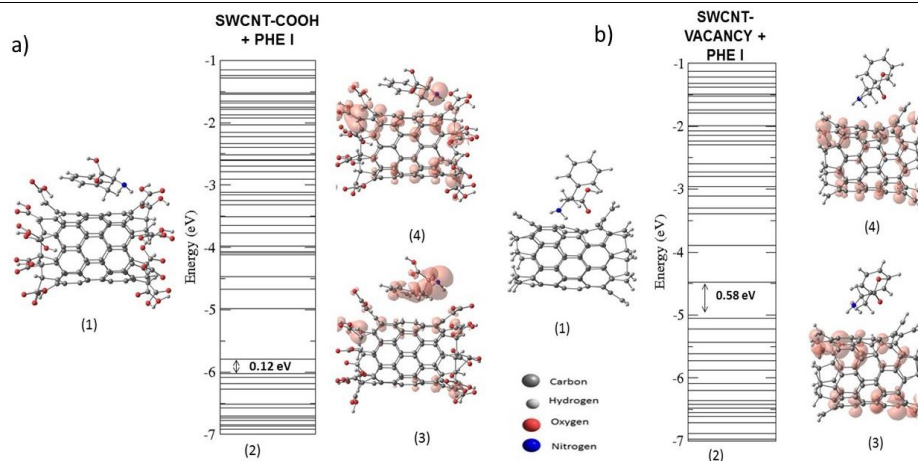
Figure 4: Most stable configurations (1), electronic levels (2), and the plot of the electronic charge density for HOMO (3) and LUMO (4) of the SWCNT-COOH (a) and SWCNT-monovacancy (b) interacting with phenylalanine. The contour plot is 0.001813 eV / $Å^3$.

The most stable configuration for the interaction between the molecules oligomycin A and Phe-F0-ATPase was I (Table 1, Figure 5), with binding energy of 6.44 eV and the shortest distance was between the oxygen atom of phenylalanine and hydrogen of oligomycin A, charge transfer was 0.16 electrons of phenylalanine towards oligomycin A, the difference between the HOMO or LUMO orbital is 0.26 eV, and the charge is concentrated on the atoms of the oligomycin A molecule nearby of the phenylalanine molecule.

The interaction between the phenylalanine and oligomycin A molecule shows high binding energy (6.44 eV) with the concentration of charges in HOMO and LUMO in both molecules. This result characterizes a chemical adsorption, stronger than the interaction between SWCNT-family members and phenylalanine residue, demonstrating that the binding energy between these residues is predominant because they are present at the active site of ATPase.
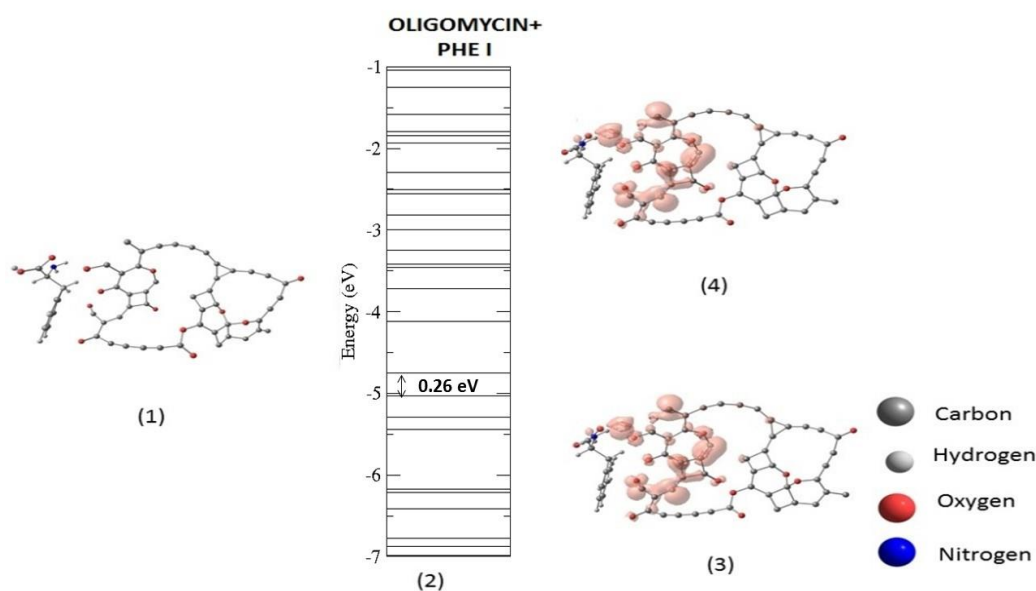

Figure 5: Stable arrangement (1), electronic levels (2) and HOMO (3) and LUMO (4) plot for the phenylalanine interacting with the oligomycin A. The contour of the charge plot is 0.001813 eV / $Å^3$.

Conclusion

In the present study we theoretically show that the use of the oxidized single-walled as SWCNT-COOH with zigzag topologies may be more efficient in preventing / inhibiting the pathological

hydrolysis from ATP based on the interaction with mitochondrial phenylalanine-F0-ATPase residues already demonstrated in previous molecular docking studies. The DFT results showed that the most stable configuration of the SWCNT-COOH and phenylalanine interaction has a binding energy of 1.79 eV, and the charge concentration occurs in the carbon nanotube and phenylalanine, which supports a chemical type adsorption. The SWCNT-OH, SWCNT-pristine, SWCNT-monovacancy configurations showed binding energies ranging from 0.37 to 0.61 eV and the charge concentration occurs only in the carbon nanotube, which supports a physical adsorption regime.

These results could be promising in the treatment of degenerative disorders where mitochondrial bioenergetic dysfunction (pathological ATP-hydrolysis) is directly involved. In this regard, these theoretical evidences can also contribute to improve the selectivity in the therapies based on mitochondrial mechanisms toward Mito-target Precision Medicine based on the detailed study of the structural and electronic properties associated to oxidized carbon nanotubes (SWCNT-COOH).

References

1. Lin MT, Beal MF (2006) Mitochondrial dysfunction and oxidative stress in neurodegenerative diseases. Nature 443: 787-795.
2. Bhat AH, Dar KB, Anees S, Zargar MA, Masood A, et al. (2015) Oxidative stress, mitochondrial dysfunction and neurodegenerative diseases; a mechanistic insight. Biomedicine & Pharmacotherapy 74 : 101-110.
3. Nikalje AP (2015) Nanotechnology and its applications in medicine. Med chem 5: 81-89.
4. Guo H, Bueler SA, Rubinstein JL (2017) Atomic model for the dimeric FO region of mitochondrial ATP synthase. Science 358: 936-940.
5. Johnson KM, Cleary J, Fierke CA, Opipari AW Jr, Glick GD (2006) Mechanistic basis for therapeutic targeting of the mitochondrial F1Fo-ATPase. ACS chemical biology 1: 304-308.
6. John AA, Subramanian AP, Vellayappan MV, Balaji A, Mohandas H, et al. (2015) Carbon nanotubes and graphene as emerging candidates in neuroregeneration and neurodrug delivery. International journal of nanomedicine 10: 4267.
7. Guo Q, You H, Yang X, Lin B, Zhu Z, et al. (2017) Functional single-walled carbon nanotubes 'CAR' for targeting dopamine delivery into the brain of parkinsonian mice. Nanoscale 9: 10832-10845.
8. Cellot G, La Monica S, Scaini D, Rauti R, Bosi S, et al. (2017) Successful Regrowth of Retinal Neurons When Cultured Interfaced to Carbon Nanotube Platforms. Journal of Biomedical Nanotechnology 13: 559-565.
9. Kohn W, Sham LJ (1965) Self-consistent equations including exchange and correlation effects. Physical review 140: A1133.
10. González-Durruthy M, Werhli AV, Cornetet L, Machado KS, González-Díaz H, et al. (2016) Predicting the binding properties of single walled carbon nanotubes (SWCNT) with an ADP/ATP mitochondrial carrier using molecular docking, chemoinformatics, and nano-QSBR perturbation theory. RSC Advances 6: 58680-58693.
11. Mehra NK, Mishra V, Jain NK (2014) A review of ligand tethered surface engineered carbon nanotubes. Biomaterials 35: 1267-1283.
12. Bevilaqua RC, Zanella I, Fagan SB (2010) Chlorophyll a and pheophytin a as gas sensors of CO_2 and O_2 molecules. Chemical Physics Letters 496: 310-315.
13. Soler JM, Artacho E, Gale JD, García A, Junquera J, et al. (2002) The SIESTA method for *ab initio* order-N materials simulation. Journal of Physics: Condensed Matter 14: 2745.
14. Perdew JP, Zunger, A (1981) Self-interaction correction to density-functional approximations for many-electron systems. Physical Review B 23: 5048-5079.
15. Troullier N, Martins JL (1991) Efficient pseudopotentials for plane-wave calculations. Physical review B 43: 1993-2006.